earth

MDPI

Article

Global Climate Classification and Comparison to Mid-Holocene and Last Glacial Maximum Climates, with Added Aridity Information and a Hypertropical Class

Brice B. Hanberry

USDA Forest Service, Rocky Mountain Research Station, Rapid City, SD 57702, USA; brice.hanberry@usda.gov

Abstract: Climate classifications supply climate visualization with inference about general vegetation types. The Köppen classification system of thermal classes and an arid class is widely used, but options are available to strengthen climate change detection. For this study, I incorporated temperature and aridity information into all climate classes to isolate climate change, added a hypertropical class to better detect warming and drying in tropical zones, and developed a consistent ruleset of thermal classes with one temperature variable for streamlined application, yet maintained primary Köppen thermal classes. I compared climate currently to 6000 years ago (ka; Mid-Holocene) and 22 ka (Last Glacial Maximum) worldwide. Growing degree days > 0 °C was the most efficient variable for modeling thermal classes. Climate classes based on growing degree days matched 86% of Köppen thermal classes. Current climate shared 80% and 23% of class assignments with the Mid-Holocene and Last Glacial Maximum, respectively, with dry conditions shifting to the tropical and hypertropical classes under current climate. Contributing to our understanding of global environmental change, this classification demonstrated that the hypertropical class experienced the greatest change in area since 6 ka and the second greatest change in area since 22 ka, and the greatest increase in percentage arid classes during both intervals. The added hypertropical class with aridity information delivered sensitive detection of warming and drying for relevant climate classes under climate change.

Keywords: class; climate change; education; GIS; growing degree day; Köppen; tutorial

Citation: Hanberry, B.B. Global Climate Classification and Comparison to Mid-Holocene and Last Glacial Maximum Climates, with Added Aridity Information and a Hypertropical Class. *Earth* **2023**, *4*, 552–569. https://doi.org/10.3390/earth4030029

Academic Editor: Charles Jones

Received: 30 June 2023
Revised: 24 July 2023
Accepted: 24 July 2023
Published: 27 July 2023

1. Introduction

Climate classifications effectively compress climate information into climate units, which have general agreement with physiological tolerances of dominant vegetation at different latitudes, allowing inference about climate and climate change effects on vegetation [1,2]. Köppen (1884; Ref. [3]) developed the first and most widely used climate classification system based on primary thermal classes and a differentiated arid class; these classes are subdivided based on additional temperature and precipitation conditions by seasons or number of months [4]. The classification system has not been static and continued refinements have occurred to better fit vegetation [4–6]. Alternative classification systems have been proposed; for example, Thornthwaite (1948; Ref. [7]) suggested a classification system that relied on the relationship between precipitation and evapotranspiration, which was realized by Feddema (2005; Ref. [8]).

Potential improvements to the Köppen classification system can increase information dissemination and climate change detection, particularly by disentangling temperature and precipitation and subdividing large tropical areas. Both aridity and temperature are equally critical information; therefore, the main drawback to the Köppen classification system is an arid class that discards primary thermal class information. In the Köppen system, once aridity is determined by applying one of various threshold options [4–6], the dry or arid (B) class is separated from thermal classes (e.g., tropical, subtropical, temperate, boreal or cold, and polar), retaining only 'hot' or 'cold' as information, and so that is not clear which thermal classes are arid and which classes are changing in aridity for comparisons over time. Another issue may be that despite 30 subclasses, many subclasses represent relatively small areas worldwide; conversely, three subclasses, namely cold and no dry season (11.5% of the global land area; Table 1), tropical savanna (12.5% of the global land area), and hot arid desert (16% of global land area), cover about 40% of global land area combined. Arid classes are rare in colder thermal classes, but abundant in the tropical class, resulting in a large global area of the tropical class and embedded arid classes within the tropical class (40%). The tropical zone is near the thermal tolerances of animals and humans and even small temperature changes may produce substantial consequences [9,10], but the disproportionate extent of the tropical class with the embedded arid class obscures change detection [11]. Additionally, inconsistent subclasses occur, such as wet forests, which are limited to tropical rainforests only. These problems can be solved by clearly incorporating temperature and aridity into every class and dividing the tropical class into two classes, which will provide new applications for climate classification, in order to improve sensitivity to climate change detection.

Table 1. Thermal Köppen classes, with full subclasses, excluding the arid class, and percent area (projected to Eckert IV; from [6]), mean temperature, reduced thermal classes, and alternative ruleset based on growing degree days (GDD0 = growing degree days at base 0 °C).

Thermal Köppen Class	Subclass	% Area	°C	Reduced Thermal Class		Ruleset
Tropical, rainforest	Af	5.4	25.5	Tropical	A	GDD0 > 9250
Tropical, monsoon	Am	3.8	25.4			
Tropical, savannah	Aw	12.5	24.9			
Temperate, hot summer	Cwa	3.1	20.6	Subtropical	B	5950 < GDD0 ≤ 9250
Temperate, hot summer	Cfa	4.1	17.1			
Temperate, warm summer	Cwb	1.3	15.9			
Temperate, hot summer	Csa	1.1	15.8			
Temperate, warm summer	Csb	0.6	12.4	Temperate hot	Ch	3070 < GDD0 ≤ 5950
Cold, hot summer	Dsa	0.2	11.5			
Temperate, warm summer	Cfb	1.9	11.4			
Cold, hot summer	Dfa	1.5	9.8			
Temperate, cold summer	Cwc	0.0	8.7			
Cold, hot summer	Dwa	0.9	8.1			
Temperate, cold summer	Csc	0.0	6.9	Temperate warm	Cw	1570 < GDD0 ≤ 3070
Temperate, cold summer	Cfc	0.1	6.8			
Cold, warm summer	Dsb	0.4	6.7			
Cold, warm summer	Dfb	5.5	4.9			
Cold, warm summer	Dwb	0.9	2.6			
Cold, cold summer	Dwc	2.2	−4.9	Boreal	D	300 < GDD0 ≤ 1570
Cold, cold summer	Dfc	11.5	−4.3			
Cold, very cold winter	Dfd	0.4	−12.9			
Cold, cold summer	Dsc	1.2	−6.9			
Cold, very cold winter	Dsd	0.0	−12.2			
Cold, very cold winter	Dwd	0.2	−13.9			
Polar, tundra	Et	6.0	−10.2	Tundra	E	3 < GDD0 ≤ 300
Polar, frost	Ef	1.3	−35.8	Polar	F	GDD0 ≤ 3

In the Köppen system, both temperature and precipitation thresholds are uncertain, and different alternatives have been developed [4,6]. Primary thermal classes have poor separation in temperature due to the incorporation of seasonality; some cold thermal subclasses (i.e., cold, with hot summer) are overall warmer than some temperate subclasses (Table 1). Indeed, although not critical, other temperature and precipitation derivatives may be more explanatory [12]. For example, growing degree days, or the accumulation of temperatures typically above 0 °C or 5 °C, dictate vegetation growth, performing the same function as the cumulative month counts at different temperature thresholds that separate thermal classes in the Köppen system, but more efficiently. Identification of the most efficient temperature variable to distinctly differentiate thermal classes is a research gap currently.

Numerous indices that incorporate precipitation and evapotranspiration have been developed to determine dryness which may be more useful than variable and inconstant precipitation rules. Aridity indices that use the relationship between precipitation and evapotranspiration, or even temperature (as occurs for the determination of arid classes but not the precipitation subclasses in the Köppen system), are similar (Figure 1). One climatic moisture index has a −1 to 1 scale, which should transfer well in space and time [8]. However, the aridity index of precipitation to potential evapotranspiration appears to be well-accepted internationally, and already has arid class thresholds assigned, meaning that it is uniquely positioned as an ideal improvement for climate classification [13,14]. Liu et al. (2019; Ref. [15]) examined changes in the aridity index alone during the Mid-Holocene, about 6000 years ago (ka), compared to near-current climate.

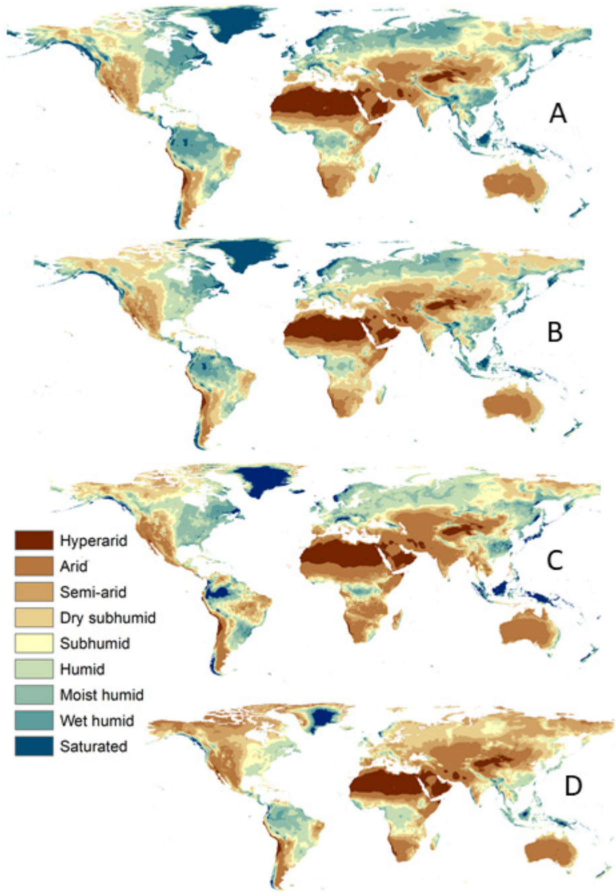

Figure 1. Aridity based on precipitation and evapotranspiration of the aridity index (**A**), climatic moisture index (**B**), Thornthwaite index (**C**), and Köppen index based on precipitation and temperature (**D**). For values (i.e., not grouped as classes), the Thornthwaite and climatic moisture indices had a correlation of 0.88, the climatic moisture and aridity indices had a correlation of 0.61, the aridity and Köppen indices had a correlation of 0.71, the aridity and Thornthwaite indices and also climatic moisture and Köppen indices had a correlation of r = 0.57, and the Thornthwaite and Köppen indices had a correlation of r = 0.27.

For past climate, Guetter and Kutzbach (1990; Ref. [5]) may have been the first to apply a Köppen climate classification system at the global scale, but for an extremely coarse spatial resolution of 4 degrees latitude by 7.5 degrees longitude. Yoo and Rohli (2016; Ref. [16]) and Willmes et al. (2017; Ref. [17]) developed global Köppen–Geiger climate maps of 21 ka, 6 ka, and the present. However, following the Köppen system, temperature and aridity were not differentiated, and class membership could shift between thermal and arid classes, resulting in unstable tracking of change over time and space, although clearly polar classes decreased as warmer classes increased with global warming since the Last Glacial Maximum.

Regarding paleoclimate, the Last Glacial Maximum, when ice sheets were at their maximum extents, occurred about 24–17 thousand years ago [18]. Since the onset of deglaciation, global warming of about 6 °C to 7 °C has occurred, primarily between 16.9 ka and 9.5 ka, with a slight warming trend of about 0.5 °C to 1 °C from 9.5 ka to 0 ka [18–20]. Aridity or available moisture depends on the balance between precipitation and evapotranspiration rates. Evapotranspiration is diminished in colder climates, both at higher latitudes under current climate and when climate was colder in the past. During the Last Glacial Maximum, a reduction in precipitation was in part compensated for by diminished evapotranspiration, but moisture balance had great spatial heterogeneity at a variety of scales [21].

The Köppen system has been altered since it was first proposed, with many potential refinements to improve correspondence with vegetation or meet other research needs. However, the Köppen system may not be sufficient to isolate changes in temperature and precipitation and the location of climate change. Specifically, if the tropical class increases in area over time due to increased temperatures while aridity also increases in the warming tropical class, the increases will obscure each other in the Köppen system. In addition, the tropical class covers a very large extent of the global land surface, which means that the overall class is not sensitive to the extreme prolonged heat that is developing in the hottest areas. Less essentially, other temperature derivatives may be equally as effective at maintaining the Köppen thermal classes and be simpler to determine than the number of months above temperature thresholds, for clear delineation of classes by temperature thresholds. Therefore, my primary objective was to demonstrate options to better detect climate change. For this, I incorporated both temperature and aridity into all climate classes to isolate information for comparisons of both temperature and aridity over time and added a hypertropical class for more sensitive climate change detection in the tropics, which are novel developments, to my knowledge. My second objective was to provide efficiency with the Köppen system for streamlined classification. In addition to the application of the aridity index, I modeled a thermal ruleset based on the primary Köppen thermal classes to allow for straightforward thermal classification using only one temperature variable, which will fill the research gap by identifying the most efficient temperature variable, and then supplied a GIS workflow and tool to rapidly group and combine the aridity and thermal classes for generating climate classes. My third objective was to display the magnitude of climate change effects in global climate classes over time. I employed climate classification with added arid information and a hypertropical class worldwide for the current climate (1960 to 1990) compared to the climate of 6000 years ago (ka) during the Mid-Holocene and 22 ka during the Last Glacial Maximum. This climate classification is sensitive to the changing climate and can demonstrate climate and climate change concepts, along with GIS as a tool, as an educational application.

2. Materials and Methods

2.1. Climate Datasets

The climate data used in this study were obtained from the global datasets from WorldClim 1.4 [22] and ENVIREM [23], with a resolution of 0.042°, or approximately ~5 km at the equator. The data for current climate, covered from 1960 to 1990, and the data for the past climate of 6 ka (Mid-Holocene) and 22 ka (Last Glacial Maximum) were from three general circulation models, namely the Community Climate System Model version 4 (CCSM4), Model for Interdisciplinary Research on Climate (MIROC-ESM), and Max Planck Institute Earth System Model (MPI-ESM-P). WorldClim data are based on interpolations among weather stations and are widely used, with over 20,000 citations for WorldClim 1.4. The variables from WorldClim 1.4 were the mean temperature, the maximum temperature of the warmest and coldest month, the minimum temperature of the coldest and warmest month, the mean temperature of the warmest quarter (i.e., three months) and coldest quarter, and annual precipitation. Variables from ENVIREM, which were calculated from WorldClim 1.4 monthly temperature and precipitation and monthly solar radiation, were growing degree days at base 0 °C (sum of the mean monthly temperature for months with a mean temperature greater than 0 °C multiplied by the number of days), growing degree days at base 5 °C, count of the number of months with a mean temperature greater than 10 °C, and the annual potential evapotranspiration.

2.2. Thermal Classes

Global Köppen classification for the current climate is available as GIS layers [6], which I used as a basis for comparison. First, I collapsed the Köppen climate classes into seven primary thermal classes by combining each primary class through reclassification of the data layer (Table 1). After projecting to Eckert IV to preserve global area, the area was calculated for each class. The annual mean temperature for each class also was determined (WorldClim 1.4; Ref. [22]).

To identify one temperature variable that facilitated streamlined classification, I modeled the relationship between the seven primary thermal classes and potential thermal metrics. The ten options were: growing degree days at base 0 °C (sum of the mean monthly temperature for months with a mean temperature greater than 0 °C multiplied by the number of days), growing degree days at base 5 °C, mean temperature, maximum temperature of the warmest and coldest month, minimum temperature of the coldest and warmest month, mean temperature of the warmest quarter (i.e., three months) and coldest quarter, and count of the number of months with a mean temperature greater than 10 °C (WorldClim and ENVIREM variables; Refs. [22,23]). For modeling, 320,000 random samples of the seven primary thermal classes were selected.

Modeling incorporated the random forest classifier to determine the most important variable and then applied the C5.0 classifier, which generates an explicit ruleset, based on the most influential variable. Although hundreds of different options for modeling classes are available [24], general linear models, MaxEnt, and random forest are the most commonly applied classifiers [25,26]. The random forest classifier may be the most accurate classifier overall [24]. Random forest is a nonlinear ensemble method, which aggregates results of many decision trees or rule-based models to output the most optimal result, helping to minimize the influence of error; the random forest classifier runs models in parallel (i.e., bagging) and averages results to reduce variance (i.e., overfitting; Ref. [27]). However, random forest is not able to generate a ruleset, but C5.0 is a similar type of algorithm that can provide classification rules. For modeling, data were partitioned into training (75% of data) and test sets (remaining data), trained with 10-fold cross-validation, and then predicted for the test sets [28,29].

To evaluate differences between the two classification systems, the percentage of thermal classes was identified that differed in assignment between the new thermal metric classification and the Köppen climate classification [6]. For mismatched classes, I compared colder classes with a global land class cover [30]. The arid Köppen climate classes were missing a thermal class assignment, but generally arid classes were warmer, producing a bias in land cover comparisons because a greater percentage of warmer thermal classes than colder classes were transferred to arid classes.

2.3. Aridity Classes

For assigning aridity classes, the aridity index (ratio of annual precipitation from WorldClim 1.4 to potential evapotranspiration from ENVIREM) was calculated. Initially, I generated nine aridity index classes, after adding non-arid classes, which produced too many final classes (Table 2). I kept the first three aridity classes of hyperarid, arid, and semi-arid, but grouped together wet humid and saturated classes and merged the remaining four middle classes. This left five classes: three dry classes, a moderate class, and a wet class.

Table 2. Aridity index for class assignments, percent area (projected to Eckert IV), precipitation (mm), potential evapotranspiration (mm), and aridity index value.

Classification	Aridity Index	% Area	Precipitation	PET	Aridity	Class
Hyperarid	<0.05	8.45	34	1823	0.02	H
Arid	0.05 to 0.20	13.11	192	1579	0.12	A
Semi-arid	0.20 to 0.50	17.58	474	1379	0.34	S
Dry subhumid	0.50 to 0.65	9.57	659	1143	0.58	M
Subhumid	0.65 to 0.80	10.56	756	1044	0.72	M
Humid	0.8 to 1.0	12.48	968	1078	0.90	M
Moist humid	1.0 to 1.25	11.63	1129	1016	1.11	M
Wet humid	1.25 to 2	12.04	1641	1068	1.54	W
Saturated	≥2	4.58	2037	724	2.81	W

2.4. Assigning Classes to Current and Past Climates

Following the C5.0 classifier ruleset for thermal classes and the aridity classes, classes were assigned and combined for the climate for 1960 to 1990 and the past climate of 6 ka (Mid-Holocene) and 22 ka (Last Glacial Maximum) according to three general circulation models, namely Community Climate System Model version 4 (CCSM4), Model for Interdisciplinary Research on Climate (MIROC-ESM), and Max Planck Institute Earth System Model (MPI-ESM-P; Tables 1 and 2, Figure 2, Supplementary files; with the same source and resolution as current climate, of WorldClim 1.4 and ENVIREM). Because arid classes were rarer in colder thermal classes, I reduced the number of arid classes to one for the polar and tundra classes and two for the boreal and temperate warm classes. The area, growing degree days at base 0 °C, and aridity index were quantified. However, the tropical class disproportionately covered a larger area (40%) and furthermore, this class is expected to increase with time. Therefore, I added a hypertropical class (at a threshold of 11,500 growing degree days at base 0 °C). Then, I compared matching classes. Additionally, I developed an ArcGIS tool (ESRI, Redding, CA, USA) for this workflow that requests three input layers of growing degree days at base 0 °C, annual precipitation, and annual potential evapotranspiration, and outputs the climate classification rapidly (Figure 2).

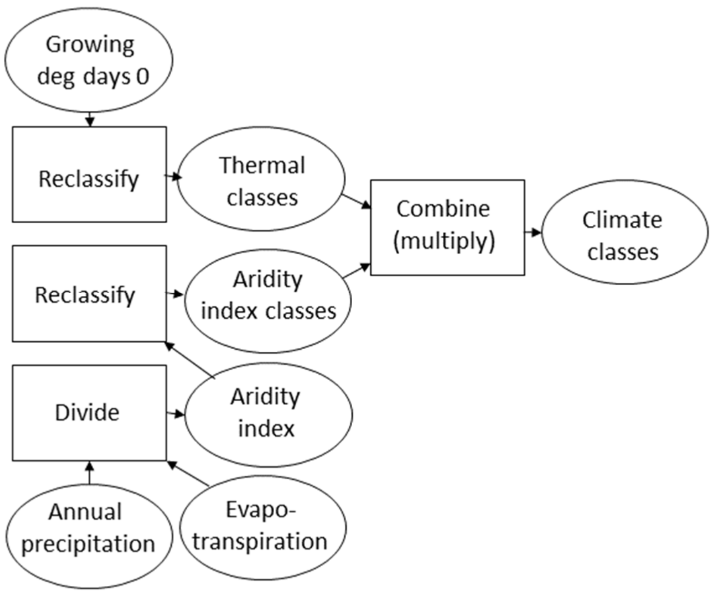

Figure 2. Streamlined steps for climate classification, including simply grouping growing degree days (base 0 °C) into classes, calculating the aridity index and grouping the aridity index values into classes, and then combining the thermal and aridity classes.

3. Results

3.1. Thermal Classes

For the modeling of thermal metrics, accuracy was 97% (predicted on withheld data) for matching the Köppen climate classes with all variables, and the two most influential variables were those for growing degree days. Accuracy was 86% (predicted on withheld data) based on the variable of growing degree days with a base of 0 °C and 83% based on the variable of growing degree days with a base of 5 °C. Therefore, I applied the simple rules for classification using growing degree days with a base of 0 °C (Table 1); distinctive separation by growing degree days occurred among the classes (Table 3). After application, the two classification systems retained an 86% match in classes based on the number of pixels that shared the same thermal classes in the growing degree day climate classification compared to the Köppen climate classification layer, which assigns thermal classes based on the number of months above different temperature thresholds (Figure 3).

Table 3. Summary of climate classification by growing degree days (GDD0) and aridity index for the current (1960–1990) climate and Last Glacial Maximum (22,000 years ago; CCSM model), with an additional hypertropical class. Thermal classes: F = polar, E= tundra, D = boreal, Cw = temperate warm, Ch = temperate hot, B = subtropical, A = tropical, Ah = hypertropical. Arid classes: H = hyperarid, A = arid, S = semi-arid, M = moderate, W = wet. Arid classes combined for polar and tundra thermal classes; hyperarid and arid combined for boreal and temperate warm thermal classes.

	Current					Last Glacial Maximum				
Class	**GDD0**	**Aridity**	**% Area**	**% Thermal**	**% Arid**	**GDD0**	**Aridity**	**% Area**	**% Thermal**	**% Arid**
FA	0	0.319	0.003	1.21	0.23	0	0.356	1.014	14.71	1.01
FM	2	1.104	0.015			0	0.878	2.865		
FW	0	8.436	1.191			0	23.713	10.831		
EA	164	0.360	0.651	4.97	0.32	98	0.365	2.000	11.48	2.00
EM	144	0.861	2.837			110	0.826	6.251		
EW	124	2.069	1.477			90	2.742	3.225		
DA	946	0.119	0.331	17.73	1.68	1029	0.115	1.159	11.94	4.18
DS	839	0.397	1.409			838	0.349	3.018		
DM	811	0.856	12.270			678	0.812	5.214		
DW	722	1.751	3.722			707	2.213	2.552		
CwA	2354	0.123	1.336	11.09	3.56	2180	0.104	2.065	5.91	3.19
CwS	2166	0.355	3.406			2113	0.331	1.127		
CwM	2096	0.832	5.364			2224	0.832	1.671		
CwW	2191	2.279	0.985			2215	1.897	1.046		
ChH	4043	0.026	0.538	9.02	4.94	4941	0.026	0.323	8.77	4.17
ChA	4277	0.137	1.642			4523	0.115	1.711		
ChS	4287	0.337	1.876			4757	0.342	2.132		
ChM	4352	0.827	3.943			4566	0.841	3.429		
ChW	4222	2.175	1.025			4339	1.787	1.177		
BH	8510	0.023	1.248	17.22	9.69	7874	0.018	5.006	23.80	12.92
BA	7959	0.124	4.238			7445	0.120	3.858		
BS	7625	0.329	4.208			7567	0.343	4.060		
BM	7708	0.841	6.075			8022	0.847	8.746		
BW	7635	1.655	1.454			7971	1.736	2.129		
AH	10,366	0.015	4.200	27.64	11.65	10,024	0.020	3.097	23.2	8.8
AA	10,355	0.113	3.487			10,276	0.120	2.204		
AS	10,400	0.348	3.964			10,183	0.356	3.547		
AM	10,588	0.856	11.192			9962	0.856	8.102		
AW	10,879	1.752	4.800			9975	1.733	6.242		
AhH	12,028	0.022	2.272	11.11	6.58	12,151	0.030	0.094	0.2	0.2
AhA	12,198	0.117	2.087			12,112	0.073	0.087		
AhS	11,948	0.354	2.217			11,599	0.300	0.008		
AhM	11,763	0.794	2.552			11,559	0.686	0.007		
AhW	11,660	1.661	1.985			11,568	1.754	0.004		

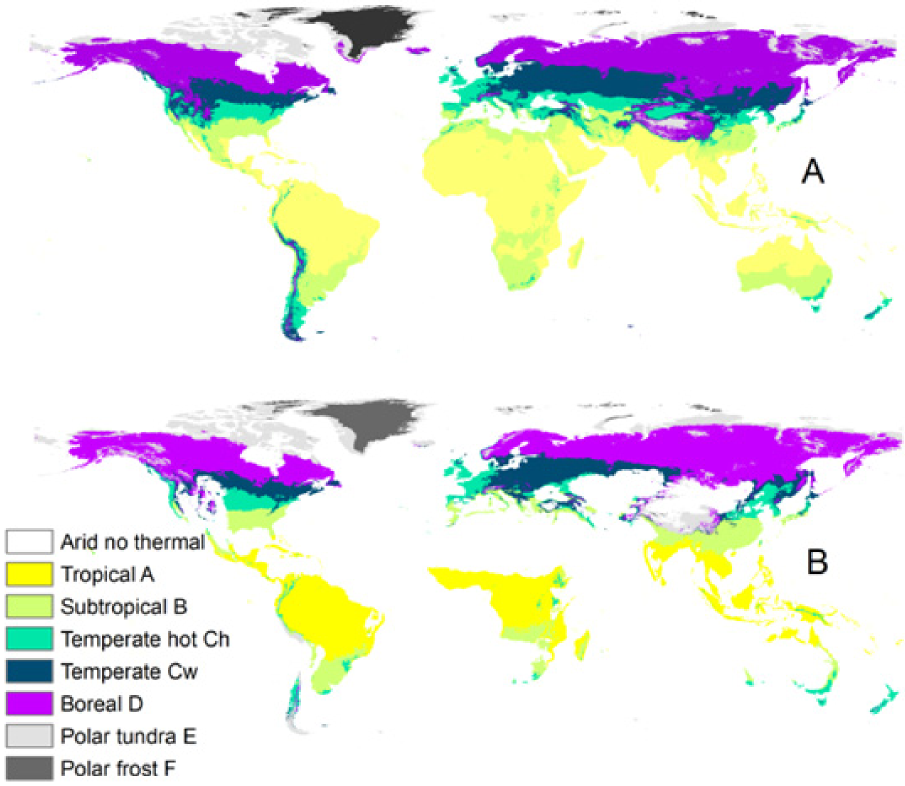

Figure 3. Primary thermal classes following growing degree days (base 0 °C; (**A**)) and following the Köppen climate classes (**B**).

The 14% of the area that did not demonstrate agreement between the two classification systems may be areas that could be classified into either class by either system equally well or even be preferable to a class according to growing degree days. The greatest difference generally in classification was the reversal of the tundra (E) class with the boreal (D) class, but based on land cover, the growing degree classification had a slightly greater percentage of lichen and tundra in the tundra class than the Köppen classification (87% compared to 81%, respectively). One of the greatest extents of disagreement occurred in northern India and China (Figure 4). Compared to the colder classes of the Köppen classification, the warmer classes based on growing degree days better aligned with agricultural use (class A and B instead of B and Ch) and also with warmer grasslands in China (class D instead of E).

3.2. Current and Past Climates

For eight primary thermal classes (i.e., after subdividing the tropical class that had about 40% of land area, using 11,500 growing degree days at base 0 °C as a threshold), the current climate (1960–1990) and climate during 6 ka shared 80% of class assignments for the CCSM4 and MPI-ESM-P general circulation models and 76% of classes for the MIROC-ESM general circulation model (Figure 5). The CCSM4 and MPI-ESM-P general circulation models shared 88% of classes, and these two general circulation models shared 80% of classes with the MIROC-ESM general circulation model. The greatest difference between current climate classes and classes of climate during 6 ka was an increase over time in the percentage of the hypertropical class, by 7 percentage points for the MIROC-ESM general circulation model and 8.5 to 9 percentage points for the CCSM4 and MPI-ESM-P general circulation models (Figure 6). Consequently, the tropical class decreased by 4 to 6 percentage points, despite gains of about 2 percentage points from the subtropical class. For current climate classes, 38.7% of classes were arid, whereas the percentage of arid classes ranged from 36.1% to 37.8% for the Mid-Holocene simulations. Although the percentage of aridity was relatively stable, the distribution of aridity changed, with the hypertropical class becoming more arid over time by about 4 percentage points (Figure 7).

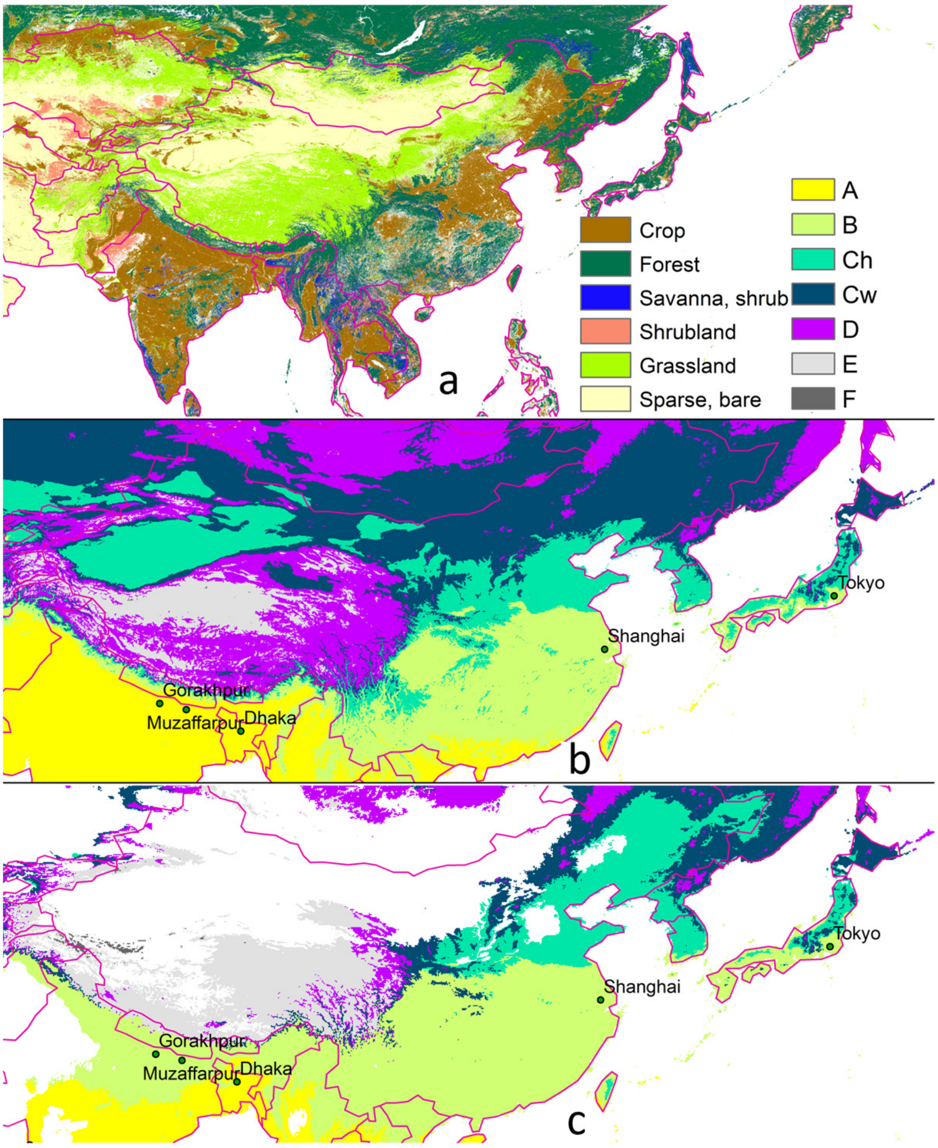

Figure 4. Primary land classes (ESA 2017) for the greatest areal extent of disagreement (**a**) between primary thermal classes following growing degree days (base 0 °C; (**b**)) and the Köppen climate classes (white areas are arid; (**c**)). Administrative boundaries are from Natural Earth (2021; Ref. [31]), but not all boundaries have agreement (https://www.naturalearthdata.com/about/disputed-boundaries-policy/) (accessed on 31 August 2021); cities have populations >1.25 million.

Current climate shared 22% to 26% of class assignments with the climate of 22 ka (Figure 8). For the Last Glacial Maximum, the CCSM4 and MPI-ESM-P general circulation models shared 68% of classes, and these two general circulation models shared 60% of classes with the MIROC-ESM general circulation model. The greatest difference between current climate classes and Last Glacial Maximum classes was a decrease in the polar class by 10.7 (MPI-ESM-P) to 13.5 percentage points (CCSM4) and an increase in the hypertropical class by 9.8 (MIROC-ESM) to 11 percentage points (CCSM4 and MPI-ESM-P; Table 3). Regarding aridity during the Last Glacial Maximum, the percentage of arid classes was about 36.5% of classes for CCSM4 and MPI-ESM-P, whereas the percentage of arid classes was 39.3% for MIROC-ESM. In the hypertropical class, the percentage of aridity increased over time by about 6 percentage points for each of the general circulation models.

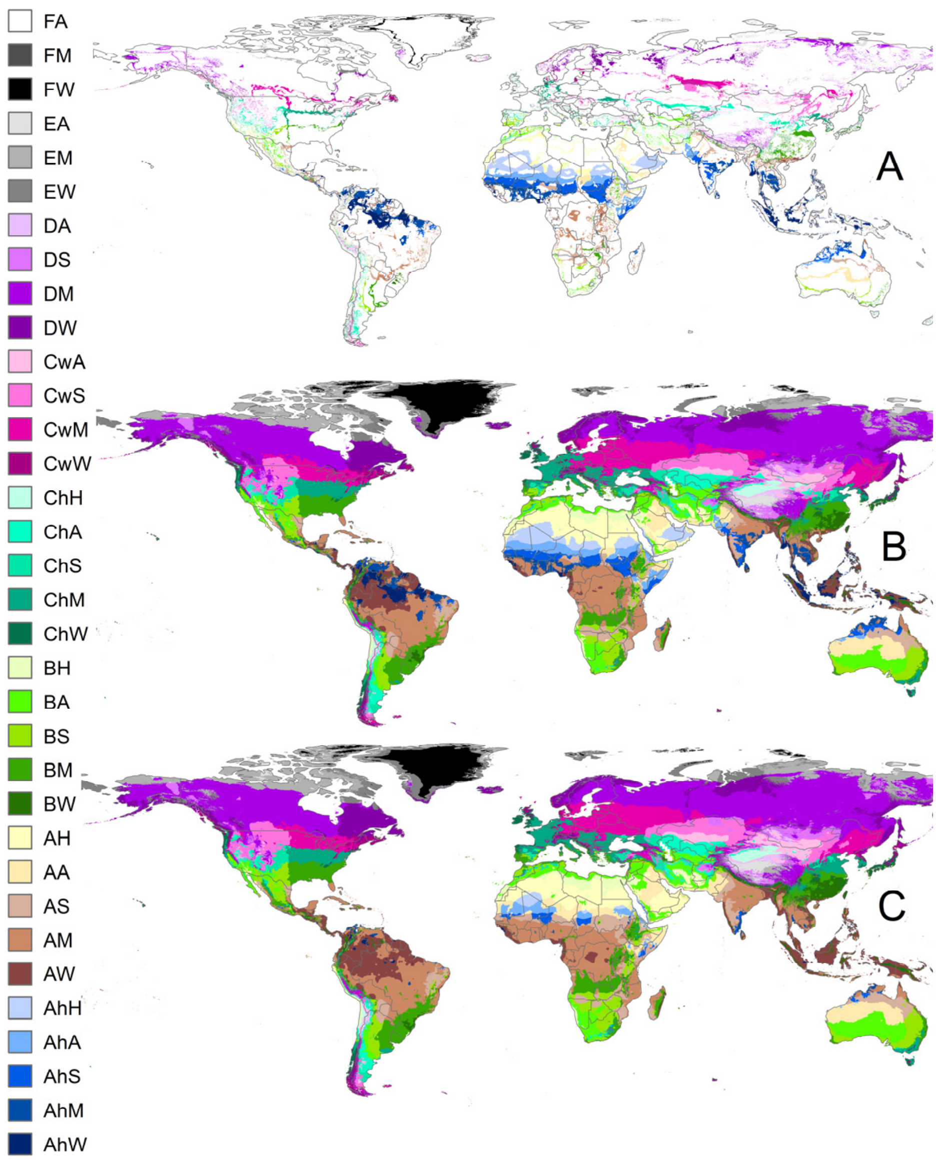

Figure 5. Classes that were different (**A**) between current climate classes (**B**) and classes from 6 ka ((**C**), CCSM4). Abbreviations are the combined thermal and arid classes. The number of arid classes is set to one for the polar and tundra classes and two for the boreal and temperate warm classes. Thermal classes: F = polar, E= tundra, D = boreal, Cw = temperate warm, Ch = temperate hot, B = subtropical, A = tropical, Ah = hypertropical. Arid classes: H = hyperarid, A = arid, S = semi-arid, M = moderate, W = wet. Administrative boundaries are from Natural Earth (2021; Ref. [31]), but not all boundaries have agreement (https://www.naturalearthdata.com/about/disputed-boundaries-policy/) (accessed on 31 August 2021).

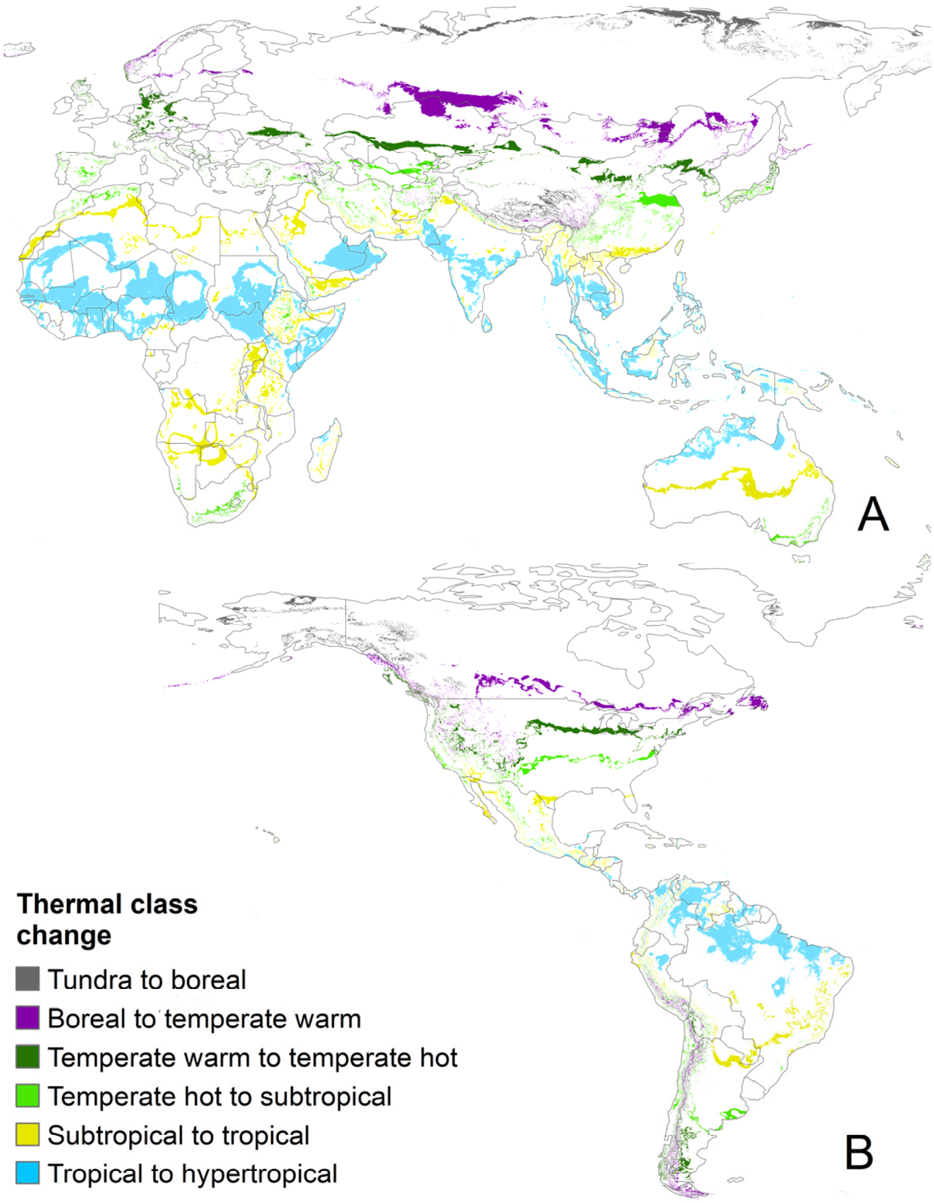

Figure 6. Changes in thermal classes between the current climate and the climate of 6 ka (CCSM4) in Africa, Asia, Europe, and Oceania (**A**) and North and South America (**B**). While most classes remained the same, the most common change was from the tropical class to the hypertropical class. Administrative boundaries are from Natural Earth (2021; Ref. [31]), but not all boundaries have agreement (https://www.naturalearthdata.com/about/disputed-boundaries-policy/) (accessed on 31 August 2021).

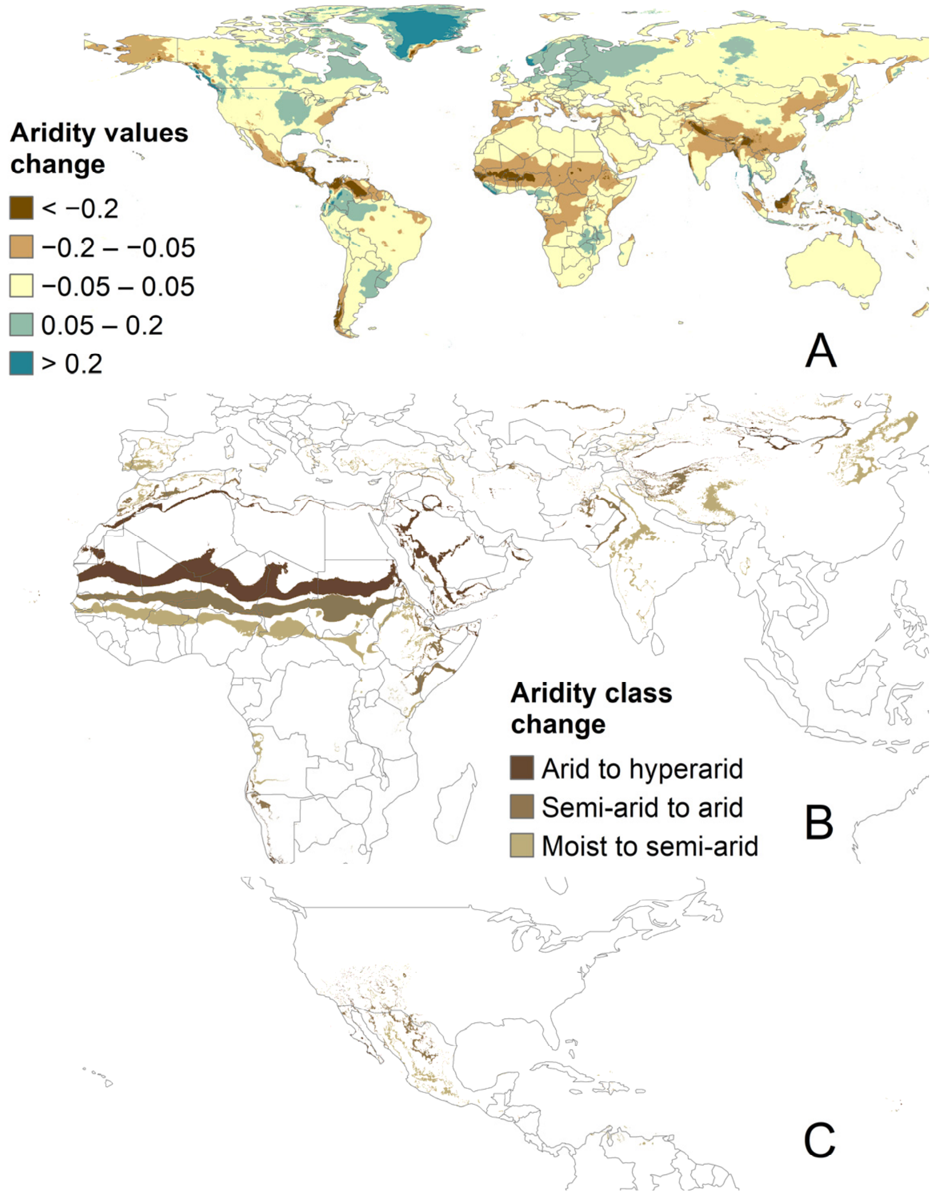

Figure 7. To isolate change in the distribution of aridity, differences in aridity index values and aridity classes between the current climate and climate of 6 ka (CCSM4) are illustrated. While most aridity index values decreased, or became more arid, in tropical zones (**A**), class changes to more arid classes were concentrated in Africa (**B**). North America displayed more class changes to increasing aridity classes than South America (**C**). Administrative boundaries are from Natural Earth (2021; Ref. [31]), but not all boundaries have agreement (https://www.naturalearthdata.com/about/disputed-boundaries-policy/) (accessed on 31 August 2021).

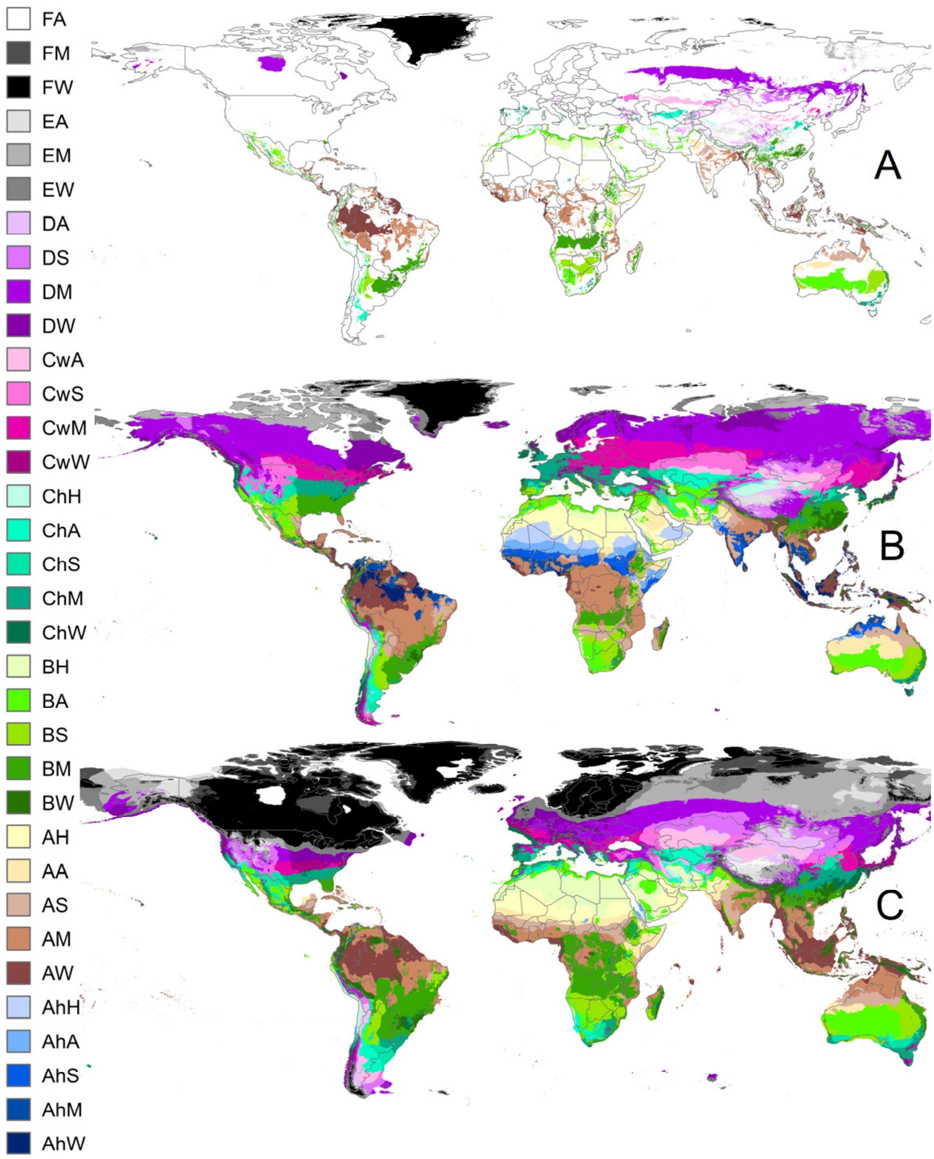

Figure 8. Classes that were the same, or no data for comparison, (**A**) between current climate classes and (**B**) classes from 22 ka ((**C**), CCSM4). Abbreviations are the combined thermal and arid classes. Arid classes to one for the polar and tundra classes and two for the boreal and temperate warm classes. Thermal classes: F = polar, E= tundra, D = boreal, Cw = temperate warm, Ch = temperate hot, B = subtropical, A = tropical, Ah = hypertropical. Arid classes: H = hyperarid, A = arid, S = semi-arid, M = moderate, W = wet. Administrative boundaries are from Natural Earth (2021; Ref. [31]), but not all boundaries have agreement (https://www.naturalearthdata.com/about/disputed-boundaries-policy/) (accessed on 31 August 2021).

4. Discussion

The Köppen system of climate classes is widely known and accepted, but has been modified over time, such as to better fit vegetation boundaries that vary with latitude [4–6]. Nonetheless, more options are available to gain information for tracking climate change over time and applying efficient GIS workflows. For example, the tropical class under current climate accounts for about 40% of all classes, although in the Köppen system, only 22% of area was in the tropical class due to removal of arid classes, which makes stable spatiotemporal comparisons of thermal class area or aridity within thermal classes impossible. One alternative option entails incorporating temperature and aridity information into all classes to allow class consistency for the comparison of climate over time, instead of partitioning all dry conditions into a dry or arid (B) class, regardless of thermal status, which affects the area of the thermal classes differentially over time. Here, I presented a streamlined system for climate classification, through efficient classification according to growing degree days and an aridity index, which delivered both temperature and aridity information to all classes and an added hypertropical class for the more sensitive detection of climate change in tropical zones, and with this system, compared global classes from current and past climates. Currently, 38.7% of climate classes are arid, and similarly, the percentage of arid classes ranged from 36.5% to 39.3% for the Last Glacial Maximum climate models and from 36.1% to 37.8% for the Mid-Holocene. Although the global arid percentage remained stable, as noted by Yoo and Rohli (2016; Ref. [16]), this classification system was able to establish that arid distribution has shifted under the current climate to the tropical and hypertropical classes since the Last Glacial Maximum and Mid-Holocene (Table 3; Figures 6 and 7). Without the additional hypertropical division and with the removal of arid-only classes, which represented about half of the tropical class, the tropical class may appear relatively stable. Guetter and Kutzbach (1990; Ref. [5]) found that, for comparisons of 18 thousand years ago (ka) to the current climate at 3000-year intervals and at 126 ka, 30% of classes never changed, with core areas that encompassed the Amazon Basin, the northern Sahara, and Australia. The northern Sahara and Australia particularly are obscured by the arid class in the Köppen system [17]. Yoo and Rohli (2016; Ref. [16]) detailed slight enlargement of the tropical wet–dry subclass area under the current climate (years 1976–2005) compared to the Mid-Holocene of 6 ka.

Overall, current climate shared 80% and 23% of class assignments with the Mid-Holocene and Last Glacial Maximum, respectively. As displayed by other global paleoclimate classification studies [16], the greatest difference between current climate classes and Last Glacial Maximum climate classes was a decrease in the polar class area, while this study revealed that the hypertropical class increased in area by almost the same percentage as the polar class area decreased. Uniquely demonstrated by this study, due to addition of the hypertropical class, the greatest difference between current climate classes and climate classes during 6 ka was an increase in the hypertropical class and a decrease in the tropical class. In contrast to the relative stability of the tropical class exhibited in the other global studies of paleoclimate classification [5,16,17], the hypertropical class showed the greatest change since 6 ka, increasing in area by 7 to 9 percentage points, and the second greatest change since 22 ka, increasing in area by 10 to 11 percentage points, and the greatest increase in the percentage of arid classes of 4 to 6 percentage points during both intervals, compared to other climate classes. The hypertropical class occurred above a threshold of 11,500 growing degree days (base 0 °C), although it did not have a strong separation from the tropical class in growing degree days. The subdivided tropical classes better detected climate change in the form of warming and drying over time than subclasses within one large tropical class and one large arid class.

Similar to the stable global arid percentage demonstrated in this study and other global studies of paleoclimate classification [16], Liu et al. (2019; Ref. [15]) also documented that the global area of drylands was similar in the Mid-Holocene to the area of drylands during the preindustrial period (approximately the year 1750), based on examining only changes in the aridity index. Liu et al. (2019; Ref. [15]) presented intense bands of decreased drylands across North Africa to the Arabian Peninsula during the Mid-Holocene compared to the climate of the preindustrial period. In chronological progression, analogous intense drylands in bands across North Africa to the Arabian Peninsula formed between the Mid-Holocene and current climate (Figure 7), as a primary contributor to increased aridity in the hypertropical class. The subdivided hypertropical class demonstrated that sensitive detection of heating and drying is possible, unlike within the large tropical and arid extents of the Köppen classification system.

Under fossil-fuel-driven pathways, warming by the end of the century may be as great as warming since the Last Glacial Maximum [19]. Greenhouse gas emissions are on a trajectory to warm global temperatures by 2–5 °C by 2100 compared to pre-industrial temperatures (circa 1850–1900), with greater warming at higher latitudes [32]. While high latitudes will experience greater warming under fossil-fuel-driven climate change, tropical classes are close to thermal extremes for animals and humans and small temperature changes may generate strong responses due to being near mortal thresholds [10,11]. Therefore, addition of the hypertropical class will make climate classification more relevant under the future climate.

Modeled climate data capture major trends of paleoclimate reconstructions, which are relatively well-known for the temperature extremes of the Last Glacial Maximum and Mid-Holocene [18–20,33]. However, climate models may not be able to fit to the climate at all locations [21], and downscaling may impose additional errors [34], resulting in differences among modeled climates. Nonetheless, the three general circulation models here produced consistent results. Precipitation patterns display greater spatial variability than temperature [21]; however, equal congruence occurred between the aridity patterns in this study and the aridity patterns displayed in Liu et al. (2019; Ref. [15]).

The Köppen system provides a link between climate and vegetation, due to the overlap that occurs between climate and biome classes with changes in temperature and latitude [1]. That is, a boreal climate class should have boreal vegetation, such as spruce (*Picea*) and larch (*Larix*) trees, a tundra climate class should contain lichen-moss, and a polar climate class should be barren, snow, and ice cover. To better fit vegetation boundaries, modifications have been applied [4–6]. Some researchers have developed alternative classification systems with other metrics or used unsupervised classification methods to cluster climate metrics [7,8,12]. Despite numerous possible variants, a useful end product needs to be generally consistent with the widely accepted and enduring Köppen system with an established connection to vegetation.

For the streamlined system using growing degree days, which was the most efficient variable for climate classification based on modeling, thermal classes were differentiated by steady increases in temperature, rather than varying with the subclass winter and summer temperatures, while remaining consistent with the primary Köppen climate classes and their established connection to biomes (Tables 1 and 3). Metzger et al. (2013; Ref. [12]) also determined that growing degree days (base 0 °C) was an effective metric for climate classification. Despite being simplified, the growing degree days classification preserved 86% of the seven primary Köppen thermal classes (i.e., polar, tundra, cold, temperate warm, temperate hot, subtropical, and tropical). Moreover, the steady increases in temperature due to classification by growing degree days (base 0 °C) may have enhanced correspondence with vegetation in the remaining 14% of classes, based on a slightly greater percentage of lichen land cover in the tundra class and better alignment with agricultural use and warmer grasslands for moderately warm classes. Although the growing degree day classification may have improved correspondence with vegetation, secondary information about seasonality was lost. In some cases, the subclasses may represent vegetation types that may be more valuable to track than the climate change information gained. Nevertheless, it certainly is possible to add the subclass information that captures the vegetation types to the combined thermal and arid classes.

The documented classification system is very flexible. The climate classification system had a total of 34 climate classes from eight thermal classes and five aridity classes, after reducing the number of aridity classes in colder thermal classes. To maintain vegetation subclasses and minimize changes, Köppen's rules of temperature and precipitation can be retained, but combined to retain both the thermal and aridity classes and the addition of the hypertropical class. Regional differences in class representation may make the merging of classes preferable for regional studies. The class thresholds for growing degree days (base 0 °C) also can be modified, for example, if a dataset has coarse temporal resolution and needs fine adjustment. Classification can occur manually, or with a tool that will output the climate classes automatically (Figure 2). Growing degree days can be exchanged for another thermal measure. Modeling then will be required for best fit, but it was possible to match 80% of growing degree day classes to the Köppen system by hand. Additionally, if preferred, other aridity thresholds can be applied or a different moisture index can replace the aridity index (ratio of annual total precipitation to potential evapotranspiration) to produce similar results (Figure 1).

For educational applications, the climate classification process would be an ideal exercise for a beginner GIS course or tutorial or a laboratory for an ecology or geography class. Climate classification can demonstrate raster and vector files, reclassifying layers, raster calculations, zonal and summary statistics, and projections. These steps can be completed manually, followed by stringing the steps together into an automatic process. Assorted data inputs may require modifications such as different projections, clipping, or units. For example, some climate layers conserve file size space via the conversion of decimals to integers. Furthermore, climate change could be demonstrated using three general circulation models.

5. Conclusions

Visualizing climate into climate units allows the conceptualization of boundaries and boundary shifts under climate change. However, current climate classification systems do not maximize information delivery, resulting in a weakness for the detection of climate change. Here, I generated information about past climate change through global climate classification, with the novel addition of a hypertropical class that is sensitive to changes in the tropical zone and differentiation of the temperature and aridity classes. Thermal classes, based on thresholds in growing degree days (base 0 °C), combined with aridity index classes supplied an efficient climate classification system. This classification system uniquely contributed to our understanding of global environmental changes, by identifying that the hypertropical class had the greatest change in area since 6 ka and the second greatest change in area since 22 ka and the greatest increase in the percentage of arid classes during both intervals. The revised climate classification system imparts the sensitive detection of warming and drying, as occurred between the Mid-Holocene and near-present climate, which will become increasingly more relevant under future climate change.

Supplementary Materials: The following supporting information can be downloaded at: https://www.mdpi.com/article/10.3390/earth4030029/s1, A symbology file and Folder S1: Seven source climate classification files of current climate (1960 to 1990) and the past climate of 6 ka (Mid-Holocene) and Last Glacial Maximum (LBM) for three general circulations models, namely the Community Climate System Model version 4 (ccsm), Model for Interdisciplinary Research on Climate (miroc), and Max Planck Institute Earth System Model (mpi).

Funding: This research received no external funding.

Data Availability Statement: These data and data comparisons were derived from the following resources available in the public domain: ENVIREM, https://deepblue.lib.umich.edu/data/concern/data_sets/gt54kn05f (accessed on 21 July 2021); WorldClim 1.4, https://www.worldclim.org/data/v1.4/worldclim14.html (accessed on 23 June 2021); Köppen climate classification, https://figshare.com/articles/dataset/Present_and_future_K_ppen-Geiger_climate_classification_maps_at_1-km_resolution/6396959/2 (accessed on 15 February 2021); global land cover, https://maps.elie.ucl.ac.be/CCI/viewer/download/ESACCI-LC-Ph2-PUGv2_2.0.pdf (accessed on 24 February 2022); the ArcGIS tool for automatic climate classification and the global climate classes for current climate are hosted at Zenodo: https://zenodo.org/record/7387289 (1 December 2022).

Acknowledgments: I thank the reviewers for their time and comments. This research was supported by the USDA Forest Service, Rocky Mountain Research Station. The findings and conclusions in this publication are those of the author and should not be construed to represent any official USDA or U.S. Government determination or policy.

Conflicts of Interest: The author declares no conflict of interest.

References

1. Rohli, R.V.; Joyner, T.A.; Reynolds, S.J.; Ballinger, T.J. Overlap of global Köppen–Geiger climates, biomes, and soil orders. *Phys. Geogr.* **2015**, *36*, 158–175. [CrossRef]
2. Hanberry, B.B.; Fraser, J.S. Visualizing current and future climate boundaries of the conterminous United States: Implications for forests. *Forests* **2019**, *10*, 80. [CrossRef]
3. Köppen, W.; Volken, E.; Brönnimann, S. Die Wärmezonen der Erde, nach der Dauer der heissen, gemässigten und kalten Zeit und nach der Wirkung der Wärme auf die organische Welt betrachtet [The thermal zones of the earth according to the duration of hot, moderate and cold periods and to the impact of heat on the organic world)]. *Meteorol. Z.* **2011**, *20*, 351–360.
4. Belda, M.; Holtanová, E.; Halenka, T.; Kalvová, J. Climate classification revisited: From Köppen to Trewartha. *Clim. Res.* **2014**, *59*, 1–13. [CrossRef]
5. Guetter, P.J.; Kutzbach, J.E. A modified Köppen classification applied to model simulations of glacial and interglacial climates. *Clim. Chang.* **1990**, *16*, 193–215. [CrossRef]
6. Beck, H.E.; Zimmermann, N.E.; McVicar, T.R.; Vergopolan, N.; Berg, A.; Wood, E.F. Present and future Köppen-Geiger climate classification maps at 1-km resolution. *Sci. Data* **2018**, *5*, 1–12. [CrossRef]
7. Thornthwaite, C.W. An approach toward a rational classification of climate. *Geogr. Rev.* **1948**, *38*, 55–94. [CrossRef]
8. Feddema, J.J. A revised Thornthwaite-type global climate classification. *Phys. Geogr.* **2005**, *26*, 442–466. [CrossRef]
9. Deutsch, C.A.; Tewksbury, J.J.; Huey, R.B.; Sheldon, K.S.; Ghalambor, C.K.; Haak, D.C.; Martin, P.R. Impacts of climate warming on terrestrial ectotherms across latitude. *Proc. Natl. Acad. Sci. USA* **2008**, *105*, 6668–6672. [CrossRef]
10. Araújo, M.B.; Ferri-Yáñez, F.; Bozinovic, F.; Marquet, P.A.; Valladares, F.; Chown, S.L. Heat freezes niche evolution. *Ecol. Lett.* **2013**, *16*, 1206–1219. [CrossRef]
11. Hanberry, B.B. Global population densities, climate change, and the maximum monthly temperature threshold as a potential tipping point for high urban densities. *Ecol. Indic.* **2022**, *135*, 108512. [CrossRef]
12. Metzger, M.J.; Bunce, R.G.; Jongman, R.H.; Sayre, R.; Trabucco, A.; Zomer, R. A high-resolution bioclimate map of the world: A unifying framework for global biodiversity research and monitoring. *Glob. Ecol. Biogeogr.* **2013**, *22*, 630–638. [CrossRef]
13. United Nations Environment Programme. World Atlas of Desertification. 1997. Available online: https://wedocs.unep.org/handle/20.500.11822/30300 (accessed on 14 February 2021).
14. Spinoni, J.; Vogt, J.; Naumann, G.; Carrao, H.; Barbosa, P. Towards identifying areas at climatological risk of desertification using the Köppen–Geiger classification and FAO aridity index. *Int. J. Climatol.* **2015**, *35*, 2210–2222. [CrossRef]
15. Liu, S.; Jiang, D.; Lang, X. Mid-Holocene drylands: A multi-model analysis using Paleoclimate Modelling Intercomparison Project Phase III (PMIP3) simulations. *Holocene* **2019**, *29*, 1425–1438. [CrossRef]
16. Yoo, J.; Rohli, R.V. Global distribution of Köppen–Geiger climate types during the Last Glacial Maximum, Mid-Holocene, and present. *Palaeogeogr. Palaeoclimatol. Palaeoecol.* **2016**, *446*, 326–337. [CrossRef]
17. Willmes, C.; Becker, D.; Brocks, S.; Hütt, C.; Bareth, G. High resolution Köppen-Geiger classifications of paleoclimate simulations. *Trans. GIS* **2017**, *21*, 57–73. [CrossRef]
18. Osman, M.B.; Tierney, J.E.; Zhu, J.; Tardif, R.; Hakim, G.J.; King, J.; Poulsen, C.J. Globally resolved surface temperatures since the Last Glacial Maximum. *Nature* **2021**, *599*, 239–244. [CrossRef]
19. Tierney, J.E.; Zhu, J.; King, J.; Malevich, S.B.; Hakim, G.J.; Poulsen, C.J. Glacial cooling and climate sensitivity revisited. *Nature* **2020**, *584*, 569–573. [CrossRef]
20. Mottl, O.; Flantua, S.G.; Bhatta, K.P.; Felde, V.A.; Giesecke, T.; Goring, S.; Grimm, E.C.; Haberle, S.; Hooghiemstra, H.; Ivory, S.; et al. Global acceleration in rates of vegetation change over the past 18,000 years. *Science* **2021**, *372*, 860–864. [CrossRef]
21. Kageyama, M.; Harrison, S.P.; Kapsch, M.L.; Lofverstrom, M.; Lora, J.M.; Mikolajewicz, U.; Sherriff-Tadano, S.; Vadsaria, T.; Abe-Ouchi, A.; Bouttes, N.; et al. The PMIP4 Last Glacial Maximum experiments: Preliminary results and comparison with the PMIP3 simulations. *Clim. Past* **2021**, *17*, 1065–1089. [CrossRef]
22. Hijmans, R.J.; Cameron, S.E.; Parra, J.L.; Jones, P.G.; Jarvis, A. Very high resolution interpolated climate surfaces for global land areas. *Int. J. Climatol. A J. R. Meteorol. Soc.* **2005**, *25*, 1965–1978. [CrossRef]
23. Title, P.O.; Bemmels, J.B. ENVIREM: An expanded set of bioclimatic and topographic variables increases flexibility and improves performance of ecological niche modeling. *Ecography* **2018**, *41*, 291–307. [CrossRef]
24. Fernández-Delgado, M.; Cernadas, E.; Barro, S.; Amorim, D. Do we need hundreds of classifiers to solve real world classification problems? *J. Mach. Learn. Res.* **2014**, *15*, 3133–3181.
25. Fourcade, Y.; Besnard, A.G.; Secondi, J. Paintings predict the distribution of species, or the challenge of selecting environmental predictors and evaluation statistics. *Glob. Ecol. Biogeogr.* **2018**, *27*, 245–256. [CrossRef]
26. Santini, L.; Benítez-López, A.; Maiorano, L.; Čengić, M.; Huijbregts, M.A. Assessing the reliability of species distribution projections in climate change research. *Divers. Distrib.* **2021**, *27*, 1035–1050. [CrossRef]
27. Breiman, L. Random forests. *Mach. Learn.* **2001**, *45*, 5–32. [CrossRef]
28. Kuhn, M. Building predictive models in R using the caret package. *J. Stat. Softw.* **2008**, *28*, 1–26. [CrossRef]
29. R Core Team. *R: A Language and Environment for Statistical Computing*; R Foundation for Statistical Computing: Vienna, Austria, 2020.
30. European Space Agency [ESA]. Land Cover CCI Product User Guide Version 2. 2017. Available online: https://maps.elie.ucl.ac.be/CCI/viewer/download/ESACCI-LC-Ph2-PUGv2_2.0.pdf (accessed on 14 February 2021).

31. Natural Earth. Downloads. 2021. Available online: https://www.naturalearthdata.com/downloads (accessed on 12 August 2021).
32. Schwalm, C.R.; Glendon, S.; Duffy, P.B. RCP8.5 tracks cumulative CO_2 emissions. *Proc. Natl. Acad. Sci. USA* **2020**, *117*, 19656–19657. [CrossRef]
33. Brown, J.L.; Hill, D.J.; Dolan, A.M.; Carnaval, A.C.; Haywood, A.M. PaleoClim, high spatial resolution paleoclimate surfaces for global land areas. *Sci. Data* **2018**, *5*, 180254. [CrossRef]
34. Beyer, R.; Krapp, M.; Manica, A. An empirical evaluation of bias correction methods for palaeoclimate simulations. *Clim. Past* **2020**, *16*, 1493–1508. [CrossRef]